

# Coupling of Neural Activity and BOLD fMRI Response: New Insights by Combination of fMRI and VEP Experiments in Transition From Single Events to Continuous Stimulation

C. Janz,<sup>1</sup> S.P. Heinrich,<sup>2</sup> J. Kornmayer,<sup>1</sup> M. Bach,<sup>2</sup> and J. Hennig<sup>1\*</sup>

**Functional magnetic resonance imaging (fMRI) measures the correlation between the fMRI response and stimulus properties. A linear relationship between neural activity and fMRI response is commonly assumed. However, the response to repetitive stimulation cannot be explained by a simple superposition of single-event responses. This might be due to neural adaptation or the hemodynamic changes underlying the fMRI BOLD response. To assess the influence of adaptation, the BOLD responses and visual evoked potentials (VEPs) to identical stimuli were recorded. To achieve different adaptation levels, 2-s stimulus epochs alternated with different interstimulus intervals (ISI = 0.0, 0.4, 0.8, 2.0, and 12 s) were presented. Neural adaptation during the checkerboard reversal paradigm used for fMRI measurements is demonstrated. Even if the measured VEP amplitude is used as the weighting function for a linear model, the measured BOLD fMRI signal time-course is not adequately predicted. Magn Reson Med 46:482–486, 2001. © 2001 Wiley-Liss, Inc.**

**Key words:** fMRI; BOLD; VEP; neural adaptation; hemodynamic response; linearity

In most functional magnetic resonance imaging (fMRI) experiments the correlation between the fMRI response and the application of a stimulus is measured. Although the nature of the complex interactions among the neurons, hemodynamic changes, and MRI is still unclear, it has been hypothesized that the fMRI response is a linear transformation of the neural activity averaged over time and voxel volume (1,2). At least for simple visual stimulation the model allows predictions of the observed blood oxygenation level dependent (BOLD) fMRI signal. While avoiding issues surrounding habituation effects by using single trials of fixed duration, sufficiently separated in time, it was shown that the BOLD fMRI response to multiple trials behaved approximately linearly (3–6). However, there is substantial literature (2,7–11) on nonlinear responses, and some disagreement on this point. Although there is evidence for neural adaptation in single cells (12) and evoked potentials (13,14), it is not clear whether the adaptation in fMRI is neural, hemodynamic, or a combination of both.

The goal of this study was to evaluate if neural adaptation is sufficient to predict the observed nonlinearity in fMRI experiments. Therefore, identical visual stimulation paradigms were presented during fMRI as well as VEP recording to assess the influence of neural adaptation on the fMRI response.

## METHODS

### Subjects

Ten healthy volunteers (four males and six females, 22–40 years old) participated in the VEP experiments, and eight healthy volunteers (six males and two females, 22–40 years old) in the fMRI experiments. Three of the subjects participated in both the VEP and fMRI experiments. All subjects provided informed consent, and the study was approved by the Institutional Review Board.

### Visual Stimulation

In all experiments a phase-reversing checkerboard pattern served as the visual stimulus. The checkerboard was confined to a circular area of 25° diameter, checksize was 1.3°, contrast 96%, and reversal rate was 4.16 Hz = 8.3 reversals/s. As the baseline condition between the stimulation units (= in the interstimulus intervals (ISI)), spatially homogenous gray stimuli were displayed with identical net luminance.

In the fMRI session the stimulation pattern was generated on a PowerMac and projected by video projector onto a backprojection screen in the magnet bore. The stimulation timing was 120 s stimulation with a fixed ISI and 60-s pause. The various ISI conditions were presented in random order. In the ISI = 0 sec condition, stimulation was continuous for 120 s. In all other ISI conditions, the stimulus was presented for 2 s, followed by an ISI of 0.4, 0.8, 2, 4, 8, or 12 s. For the VEP session the checkerboard reversal stimulus was generated by a Macintosh G4 and displayed on a CRT screen. It closely matched the stimulus used in the fMRI experiments. Six runs were averaged to increase the signal-to-noise ratio (SNR). Therefore, the ISI = 4 s and ISI = 8 s conditions were skipped to keep the overall experimental time within reasonable limits. For one experimental run, the described timing scheme was repeated five times. In the VEP and fMRI sessions all ISI sets were acquired on each subject.

### fMRI Data Acquisition

The study was performed on a 2 T whole-body system (Bruker Medspec S200 Avance) equipped with a remov-

<sup>1</sup>Section of Medical Physics, University Medical Center, Freiburg, Germany.

<sup>2</sup>Department of Ophthalmology, University Medical Center, Freiburg, Germany.

Grant sponsor: Deutsche Forschungsgemeinschaft; Grant number: DFG 1875/3-2.

\*Correspondence to: Dr. J. Hennig, Section of Medical Physics, Dept. of Radiology, Hugstetterstr. 55, 79106 Freiburg, Germany.  
E-mail: hennig@nz11.ukl.uni-freiburg.de

Received 19 December 2000; revised 11 April 2001; accepted 12 April 2001.

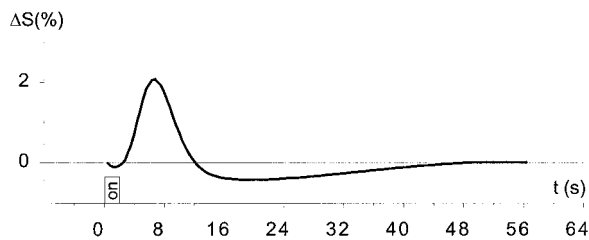


FIG. 1. Numerical representation of the hemodynamic response function after a 2-s stimulation used as the IRF. It is derived from data obtained in our previous study (10), with identical visual stimulation and experimental conditions.

able asymmetric head gradient insert with 30 mT/m gradient strength and 150 T/m/s slew rate. fMRI was performed using single-shot GE-EPI. The sequence parameters were: matrix size =  $64 \times 64$ ; FOV =  $256 \times 256$  mm<sup>2</sup>; slice thickness = 5 mm; bandwidth = 200 kHz;  $\alpha = 45^\circ$ ,  $TE_{\text{eff}} = 40$  ms, and TR = 400 ms. Three oblique slices along the calcarine fissure, prescribed in a  $T_2$ -weighted sagittal scout image, were acquired continuously: 20 initial dummy scans to reach a steady-state MR signal; 20 prestimulation baseline scans; 430 scans during one functional run; and 20 poststimulation baseline scans.

#### fMRI Analysis

The activated volume of interest (VOI) was determined in a blocked time series experiment with on/off timing of 20/40 s, which was performed in the same session. All pixels with  $P$  values less than 0.02 (Student's  $t$ -test) were considered as activated. For all experiments the mean time-courses of the relative signal change within these VOIs were calculated and first-order baseline corrected. The baseline was determined by a linear regression of the pre- and poststimulation baseline scans.

To estimate the accuracy of a linear transform model, a series of Dirac-delta functions describing the stimulus timing was convolved with the temporal fMRI impulse response function (IRF). Thus, the response to 120-s continuous stimulation is predicted as the time-shifted sum of the response to 60 2-s stimulation pulses. The numerical representation of the IRF after a 2-s stimulation (Fig. 1) was derived from data obtained in our previous study (10) and normalized to the first positive BOLD amplitude of the ISI = 12-s run.

#### EEG/VEP Data Acquisition

Visual evoked potentials (VEPs) were recorded at the occipital pole (Oz, according to standard nomenclature (15)) referenced to linked earlobes. Signals were amplified, bandpassed at 1–100 Hz, digitized at 500 Hz, and written to disk for off-line analysis. The vertical electrooculogram (EOG) was measured to detect eye blinks with a threshold criterion of 100  $\mu$ V.

#### EEG/VEP Analysis

In VEP measurements, recordings with a stimulation rate of eight reversals/s and higher are termed “steady-state”

VEPs. A standard procedure for analyzing steady-state VEPs is detecting response in the frequency domain, since the relevant frequencies are predetermined by the stimulation rate. This principle was adopted for the present study.

After eye blink rejection, three to six steady-state epochs remained for each subject and each ISI. These epochs were averaged to improve the SNR for further processing. The first 120 ms of each stimulation period were discarded. Amplitudes corresponding to the reversal rate of the stimulus (8.3 Hz) and the second harmonic (16.6 Hz) were obtained by discrete Fourier transform. These values were corrected for noise (16) and summed to yield an estimate of the stimulus-related neural activity. This sum of corrected amplitudes is defined as “VEP amplitude.” Completing this procedure for each 2-s steady-state epoch reveals how the VEP amplitude evolves over a 2-min stimulation sequence. Interindividual normalization was attained by division of the VEP-amplitude estimates by the average VEP-amplitude value across all ISIs for each subject. Noise correction may occasionally lead to a zero VEP-amplitude estimate in cases of small SNRs, resulting in an artificial distribution of values in the low VEP amplitude range. To account for this, the median rather than the mean was chosen to combine the results of different subjects.

## RESULTS

### fMRI Experiments

For all subjects a volume of activated pixels (VOI) could be determined by performing the blocked fMRI experiment in advance. The mean number of pixels in the VOI was  $102 \pm 14$  ( $\equiv 8.16 \pm 1.12$  ml) within the striate visual cortex.

Figure 2 shows the signal time-courses for the different ISIs averaged across the VOIs of all subjects. Comparison of all the fMRI signal time-courses shows an identical slope within the first 8 s after the onset of the stimulation period. For all ISI conditions a maximum signal change of 1.2–2.9% can be seen after approximately 10 s. These observed maximum signal changes are not significantly different for the ISI conditions shorter than 2 s, and are overestimated by the predictions of a linear transform model. For these ISI conditions a steady-state signal change ( $BOLD_{\text{ss}}$ , see Table 1) is established after approximately 40 s. The mean signal changes do not differ significantly between these conditions, nor do the maximum amplitudes of the poststimulus undershoot ( $BOLD_{\text{under}}$ ) and the reduction from the initial overshoot to the steady-state signal change ( $BOLD_{\text{reduc}}$ ). For ISI = 2 and 12 s, a linear response predicts the data within experimental errors.

### VEP Experiments

The median time-course of the steady-state VEP amplitude is displayed in Fig. 3. For all but the 12-s ISI, two sections can be recognized: an initial increase in the VEP amplitude with a maximum after approximately the second stimulation unit is most prominent in the 0.4-s ISI condition. The remaining curve shows a continuous decline, which can be described by an exponential with a time constant of

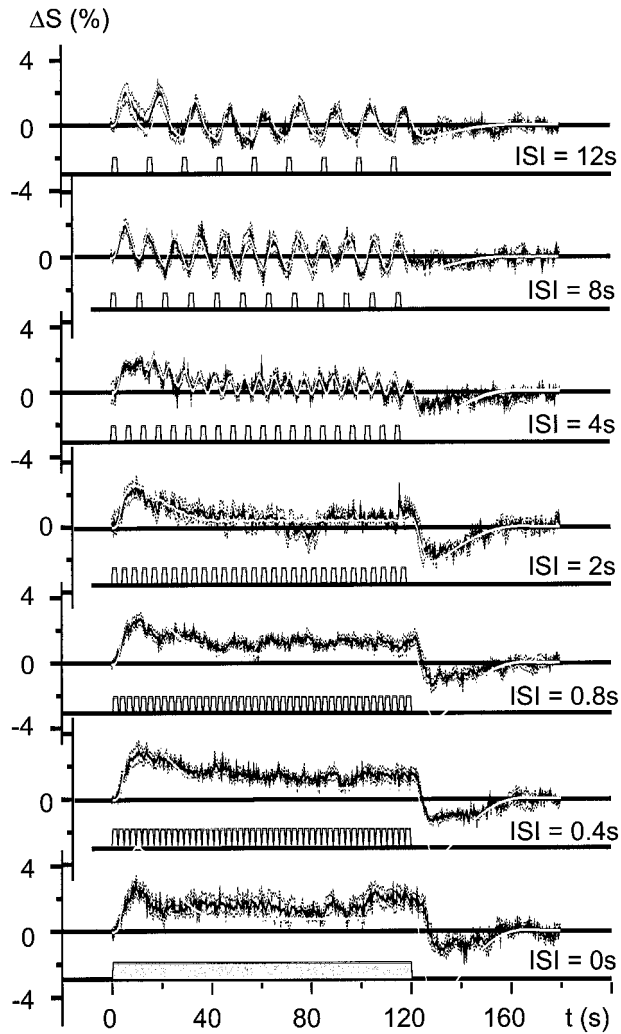


FIG. 2. Signal time-courses for the different ISIs averaged across all subjects (mean  $\pm$  SE) and its prediction by a linear transformation (gray line). The periods of stimulation are plotted on the bottom.

14.7  $\pm$  2.1 s (ranging from 13.0 to 16.6 s). The 12-s ISI condition produced a shallow curve, which can be interpreted as a sequence of “first” points, each resembling the very first low value observed with the other ISIs.

Combination of fMRI and VEP Experiments

Figure 4 shows all the estimates (dotted lines) of the signal time-courses by a convolution of the total IRF and the

Table 1  
fMRI Signal Changes During and After the Stimulation Period

ISI	BOLD <sub>ss</sub>	BOLD <sub>reduc</sub>	BOLD <sub>under</sub>
0	1.51 $\pm$ 0.04	1.27 $\pm$ 0.19	1.28 $\pm$ 0.10
0.4	1.34 $\pm$ 0.02	1.10 $\pm$ 0.21	1.35 $\pm$ 0.07
0.8	1.25 $\pm$ 0.02	1.37 $\pm$ 0.12	1.40 $\pm$ 0.16
2	0.25 $\pm$ 0.04	1.68 $\pm$ 0.10	2.15 $\pm$ 0.13

ISI, Interstimulus Interval; BOLD<sub>ss</sub>, BOLD steady state signal change (mean  $\pm$  SE); BOLD<sub>reduc</sub>, reduction of the maximum signal change to the BOLD steady state signal change (mean  $\pm$  SE); BOLD<sub>under</sub>, post-stimulus undershoot amplitude (mean  $\pm$  SE).

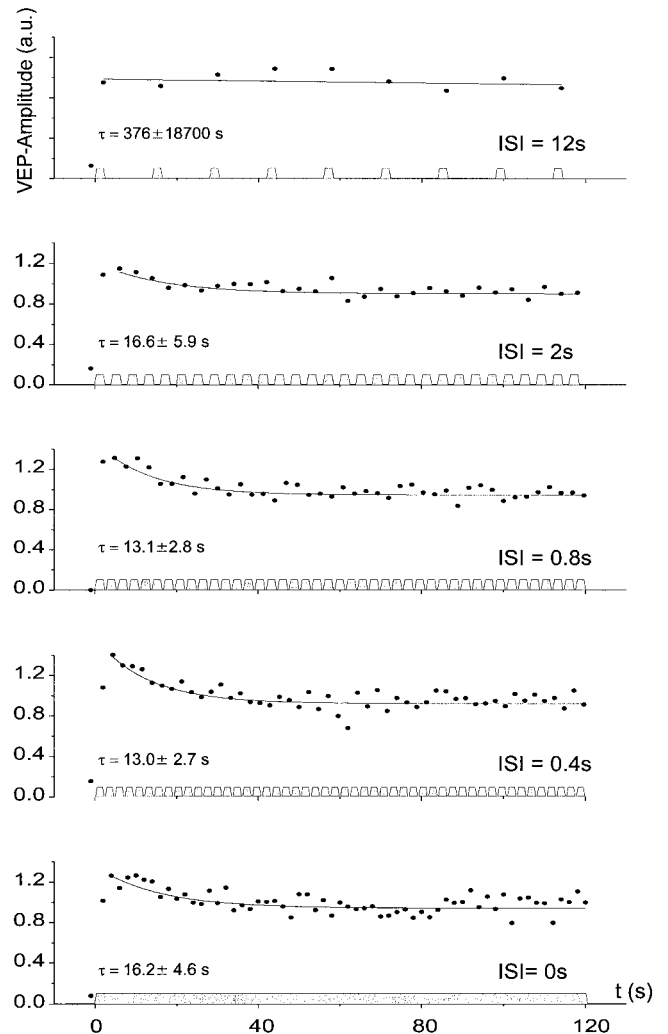


FIG. 3. The median time-course of the steady-state VEP amplitude for the different ISIs. For all but the 12-s ISI two sections can be recognized: a maximum reached after approximately the second stimulation unit, and a continuous exponential decline with a time constant of 14.7  $\pm$  2.1 s. The periods of stimulation are plotted on the bottom.

Dirac-delta stimulation input functions weighted by the VEP amplitudes. Comparison of these estimates with the measured signal time-courses (bold lines) still shows a mismatch, especially of the transient amplitudes.

DISCUSSION

Response Linearity

Even though the hemodynamic events are already interacting for ISIs longer than 2 s, the results of our fMRI experiments demonstrate that the measured response function can be predicted reasonably well by the linear superposition of single-event responses. For ISIs shorter than 2 s, however, this linear prediction becomes inaccurate. This finding is in good agreement with the results of Huettel et al. (17).

Since the impulse response function (IRF) was taken from our previous study, it could be an inappropriate

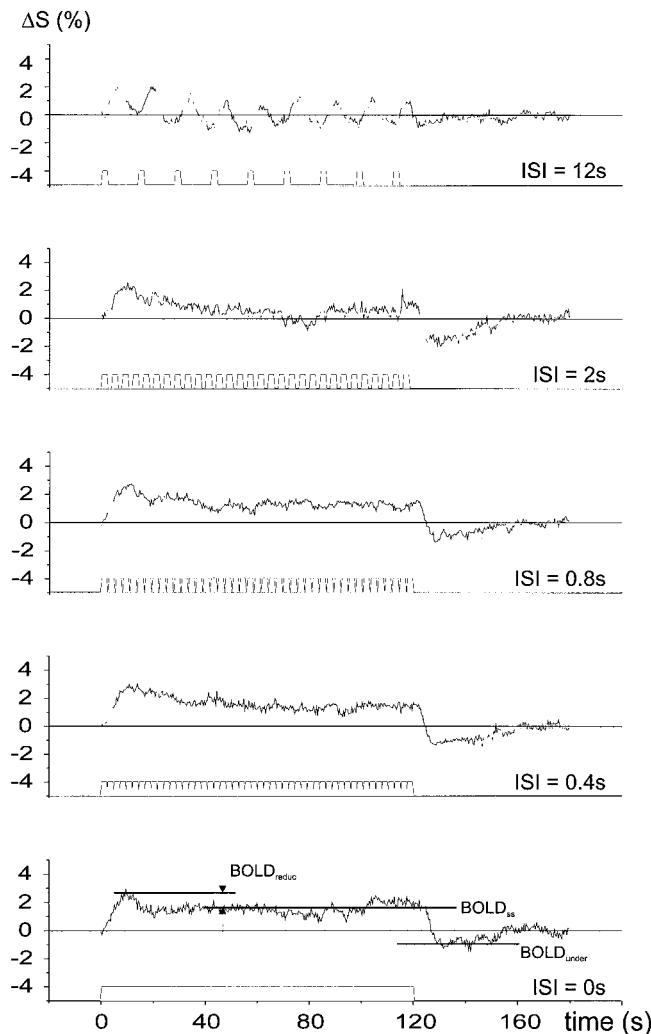


FIG. 4. Comparison of the VEP amplitude-weighted stimulation input function convolved with the IRF (gray lines) with the measured fMRI signal time-course (black lines). These predictions still overestimate the transient amplitude for ISIs of 2 s and less. The periods of stimulation are plotted on the bottom.

template for the present analysis. Some studies have shown that IRFs may vary depending on the stimulus applied and the region under observation (10,18), which can result in a better prediction of data acquired during continuous stimulation. However, the experimental conditions were identical to the earlier study (10). Additionally, to evaluate the influence of subject selection, the IRF used was tested by a correlation of the model prediction with the 12-s ISI. Any variation of the IRF undershoot deteriorated the correlation.

#### VEP Measurements and Neural Adaptation

Despite the observed nonlinearity, the hemodynamic changes during rapid neural firing might still be linearly coupled with the neural activity. Assuming a linear coupling, the nonlinearity has to be attributed to neural adaptation. Boynton et al. (2) attributed the overestimation of the maximum positive amplitude to neural adaptation

during persistent stimulation. Their data were described best weighting the input function with an exponential time constant of 1 s and a ratio of the peak response to the asymptotic response of 3 : 1. However, the parameters of neural adaptation have been derived assuming a linear coupling and were not determined experimentally.

The VEP amplitudes measured in our experiments show a time constant of approximately 15 s and a ratio of the peak response to the asymptotic response of 1.4 : 1. These data agree with Ho and Berkeley (13) and Peachey et al. (14). Weighting the stimulus input function with this adaptation does not significantly improve the prediction of the data with a linear model. The amplitudes of the transients in the signal time-courses are still overestimated (see Fig. 4). Therefore, neural adaptation alone cannot cause the observed nonlinear behavior. It has to be dominated by the nonlinear coupling of the rCBF, rCBV, and  $CMRO_2$  changes (19,20) underlying the fMRI BOLD response. This is supported by the independence of the signal changes from the integrated neural activity over time for ISIs of 2 s and below.

The measured VEP amplitudes depend on the population of neurons firing and their orientation to the surface of the head. Hence, changes in the VEP amplitude may reflect spatiotemporal changes in the activated neuronal population rather than neural adaptation (13). The amplitude of the VEP signals per se is therefore only a poor measure of the neural activity. However, as long as the activated neuronal population does not change and the tissue conductivity remains constant, it is justifiable to take the VEP amplitude as a measure of the neural activity (21). For the simple and well-studied activation paradigm used in this study, these conditions were met. Changes in the tissue conductivity as a consequence of the ionic flux occur on a much shorter timescale and may contribute to the signal fluctuations within the first 50–100 ms, which were discarded in our measurements.

## CONCLUSIONS

In this study, neural adaptation during a checkerboard reversal paradigm used for fMRI measurements was demonstrated. Even if the measured VEP amplitude is used as the weighting function for a linear model, the measured BOLD fMRI signal time-course is not adequately predicted. The BOLD signal following a brief stimulus is the result of the interaction of temporal changes in rCBF, rCBV, and  $CMRO_2$ . The observed nonlinearity of the overall signal may be caused by the different time constants of the parameters as well as hemodynamic saturation effects.

## REFERENCES

1. Friston KJ, Jezzard P, Turner R. Analysis of functional MRI time series. *Hum Brain Mapp* 1994;1:153–171.
2. Boynton GM, Engel SA, Glover GH, Heeger DJ. Linear systems analysis of functional magnetic resonance imaging in human V1. *J Neurosci* 1996;16:4207–4221.
3. Buckner RL, Bandettini PA, O'Craven KM, Savoy RL, Petersen SE, Raichle ME, Rosen BR. Detection of cortical activation during averaged single trials of a cognitive task using functional magnetic resonance imaging. *Proc Natl Acad Sci USA* 1996;93:14878–14883.

4. Janz C, Speck O, Hennig J. Time-resolved measurements of brain activation after a short visual stimulus: new results on the physiological mechanisms of the cortical response. *NMR Biomed* 1997;10:222–229.
5. Dale AM, Buckner RL. Selective averaging of rapidly presented individual trials using fMRI. *Hum Brain Mapp* 1997;5:329–340.
6. Burock MA, Buckner RL, Woldorff MG, Rosen BR, Dale AM. Randomized event-related experimental designs allow for extremely rapid presentation rates using functional MRI. *Neuroreport* 1998;9:3735–3739.
7. Vazquez AL, Noll DC. Nonlinear aspects of the BOLD response in functional MRI. *Neuroimage* 1998;7:108–118.
8. Robson MD, Dorosz JL, Gore JC. Measurements of the temporal fMRI response of the human auditory cortex to trains of tones. *Neuroimage* 1998;7:185–198.
9. Buxton RB, Wong EC, Frank LR. Dynamics of blood flow and oxygenation changes during brain activation: the balloon model. *Magn Reson Med* 1998;39:855–864.
10. Janz C, Schmitt C, Speck O, Hennig J. Comparison of the hemodynamic response to different visual stimuli in single-event and block stimulation fMRI experiments. *J Magn Reson Imaging* 2000;12:708–714.
11. Liu H, Gao J. An investigation of the impulse functions for the nonlinear BOLD response in functional MRI. *Magn Reson Imaging* 2000;18:931–938.
12. Maddess T, McCourt ME, Blakeslee B, Cunningham RB. Factors governing the adaptation of cells in area 17 of the cat visual cortex. *Biol Cybern* 1988;59:229–236.
13. Ho WA, Berkley MA. Evoked potential estimates of the time course of adaptation and recovery to counterphase gratings. *Vision Res* 1988;28:1287–1296.
14. Peachey NS, DeMarco Jr PJ, Ubilluz R, Yee W. Short-term changes in the response characteristics of the human visual evoked potential. *Vision Res* 1994;34:2823–2831.
15. American Encephalographic Society. Guideline thirteen: guidelines for standard electrode position nomenclature. *J Clin Neurophys* 1994;11:111–113.
16. Bach M, Meigen T. Do's and don'ts in Fourier analysis of steady-state potentials. *Doc Ophthalmol* 1999;99:69–82.
17. Huettel SA, McCarthy G. Evidence for a refractory in the hemodynamic response to visual stimuli as measured by MRI. *Neuroimage* 2000;11:547–553.
18. Chen W, Zhu XH, Kato T, Andersen P, Ugurbil K. Spatial and temporal differentiation of fMRI BOLD response in primary visual cortex of human brain during sustained visual stimulation. *Magn Reson Med* 1998;39:520–527.
19. Mandeville JB, Marota JJA, Ayata C, Moskowitz MA, Weisskoff RM, Rosen BR. MRI measurement of the temporal evolution of relative CMRO<sub>2</sub> during rat forepaw stimulation. *Magn Reson Med* 1999;42:944–951.
20. Mandeville JB, Marota JJA, Ayata C, Zaharchuk G, Moskowitz MA, Weisskoff RM, Rosen BR. Evidence of a cerebrovascular postarteriole windkessel with delayed compliance. *J Cereb Blood Flow Metab* 1999;19:679–689.
21. Ducati A, Fava E, Motti EDF. Neuronal generators of the visual evoked potentials: intracerebral recording in awake humans. *Electroenceph Clin Neurol* 1988;71:89–99.